MCB
Journals.ASM.org

Unraveling the Complexities of DNA-Dependent Protein Kinase Autophosphorylation

Jessica A. Neal,[a] Seiji Sugiman-Marangos,[b] Pamela VanderVere-Carozza,[c] Mike Wagner,[c,d] John Turchi,[c,e] Susan P. Lees-Miller,[f] Murray S. Junop,[b] Katheryn Meek[a]

College of Veterinary Medicine, Department of Microbiology and Molecular Genetics, and Department of Pathobiology and Diagnostic Investigation, Michigan State University, East Lansing, Michigan, USA[a]; Department of Biochemistry and Biomedical Sciences, McMaster University, Hamilton, Ontario, Canada[b]; Department of Medicine, Indiana University School of Medicine, Indianapolis, Indiana, USA[c]; Department of Pharmacology and Toxicology, Indiana University School of Medicine, Indianapolis, Indiana, USA[d]; Departments of Biochemistry and Molecular Biology, Indiana University School of Medicine, Indianapolis, Indiana, USA[e]; Departments of Biochemistry and Molecular Biology and Oncology, University of Calgary, Calgary, Alberta, Canada[f]

DNA-dependent protein kinase (DNA-PK) orchestrates DNA repair by regulating access to breaks through autophosphorylations within two clusters of sites (ABCDE and PQR). Blocking ABCDE phosphorylation (by alanine mutation) imparts a dominant negative effect, rendering cells hypersensitive to agents that cause DNA double-strand breaks. Here, a mutational approach is used to address the mechanistic basis of this dominant negative effect. Blocking ABCDE phosphorylation hypersensitizes cells to most types of DNA damage (base damage, cross-links, breaks, and damage induced by replication stress), suggesting that DNA-PK binds DNA ends that result from many DNA lesions and that blocking ABCDE phosphorylation sequesters these DNA ends from other repair pathways. This dominant negative effect requires DNA-PK's catalytic activity, as well as phosphorylation of multiple (non-ABCDE) DNA-PK catalytic subunit (DNA-PKcs) sites. PSIPRED analysis indicates that the ABCDE sites are located in the only contiguous extended region of this huge protein that is predicted to be disordered, suggesting a regulatory role(s) and perhaps explaining the large impact ABCDE phosphorylation has on the enzyme's function. Moreover, additional sites in this disordered region contribute to the ABCDE cluster. These data, coupled with recent structural data, suggest a model whereby early phosphorylations promote initiation of nonhomologous end joining (NHEJ), whereas ABCDE phosphorylations, potentially located in a "hinge" region between the two domains, lead to regulated conformational changes that initially promote NHEJ and eventually disengage NHEJ.

Classical nonhomologous end joining (c-NHEJ) is the major DNA double-strand break repair (DSBR) pathway in all vertebrates and is active throughout the cell cycle (1, 2); another important DSBR pathway, homologous recombination (HR), is active only in the S and G_2 phases of the cell cycle when a sister chromatid is available as a repair template (2). If c-NHEJ is disabled, DNA double-strand breaks (DSBs) can still be directly ligated by an alternative end joining pathway (a-NHEJ); although a-NHEJ is slower and more error prone than c-NHEJ, joining via a-NHEJ is still relatively efficient (3). VDJ recombination is the site-specific DNA recombination process that facilitates assembly of functional exons encoding the antigen binding domain of immunoglobulins and T cell receptors in developing lymphocytes. If c-NHEJ is disabled, rejoining of VDJ intermediates is severely impaired because the breaks are restricted from joining by a-NHEJ via a poorly understood mechanism (4).

The DNA-dependent protein kinase (DNA-PK) initiates the process of c-NHEJ first by utilizing the regulatory DNA binding subunit, Ku, to bind to DNA double-strand breaks (DSBs) and then by regulating access to DSBs via a series of phosphorylations mediated by the large catalytic subunit, DNA-PKcs. To date, more than 60 serines and threonines (1.5% of the 4,128 residues) within DNA-PKcs have been shown to be targeted (mostly) by DNA-PKcs itself (5, 6). Of these ~60 phosphorylation sites, 20 have been studied by mutagenesis, and 16 of those were shown to affect biological function (7–13). Of these 16 biologically relevant sites, phosphorylations of three affect enzymatic activity. Phosphorylations of the remaining 13 sites do not affect enzymatic activity. Blocking phosphorylation of some sites results in a radiosensitive phenotype, whereas at other sites, phosphomimicking results in increased radiosensitivity. These data suggest that certain autophosphorylations promote c-NHEJ (perhaps committing DSBs to the c-NHEJ pathway) while other phosphorylations function to disengage c-NHEJ, a beneficial outcome if DNA-PK were bound to a DNA end that could (or should) not be joined by c-NHEJ (for instance, an intermediate generated by repair of a DNA interstrand cross-link or a DNA end that results from replication fork arrest).

We have shown previously that autophosphorylation within two major clusters reciprocally regulates DNA end processing during c-NHEJ (10). Phosphorylation within the ABCDE cluster (including six sites between residues 2609 and 2647) promotes DNA end processing, whereas phosphorylation within the PQR cluster (including five sites between residues 2023 and 2056) limits end processing. This reciprocal regulation of end processing was surmised by sequencing repaired DSBs from cells expressing DNA-PKcs that could not be phosphorylated at either the ABCDE or PQR sites (10). Consistent with this interpretation, a mutant

Received 25 November 2013 **Returned for modification** 1 January 2014
Accepted 26 March 2014
Published ahead of print 31 March 2014
Address correspondence to Katheryn Meek, kmeek@msu.edu.
Supplemental material for this article may be found at http://dx.doi.org/10.1128/MCB.01554-13.
Copyright © 2014, American Society for Microbiology. All Rights Reserved.
doi:10.1128/MCB.01554-13

with all six ABCDE sites converted to alanines (ABCDE>Ala) blocks DNA end access *in vitro* to a variety of enzymes (14, 15) and cannot activate the Artemis nuclease (16). Although phosphorylation of the ABCDE sites clearly promotes kinase dissociation (17), ABCDE phosphorylation is neither necessary nor sufficient for kinase dissociation; we have suggested that phosphorylation of additional sites (likely in conjunction with ABCDE phosphorylation) facilitates disassembly of the complex, underscoring the complexities of how c-NHEJ is regulated by DNA-PK. Although studies from our laboratories demonstrate that phosphorylations within the ABCDE cluster are predominately autophosphorylations (18), other investigators have concluded that ATM or ATR targets these sites (19, 20).

Unlike any other DNA-PKcs mutation studied to date, blockade of ABCDE phosphorylation by mutation results in a severe cellular phenotype, consistent with ABCDE>Ala exerting a dominant negative effect on other DSB repair pathways. In fact, expressing the ABCDE>Ala mutant renders cells hypersensitive to a variety of DNA damaging agents including ionizing radiation (IR), etoposide, mitomycin C, zeocin, hydroxyurea (HU), methyl methanesulfonate (MMS), UV, cisplatin, and camptothecin (Fig. 1) (21). Recent studies from Zhang and colleagues, where alanine substitutions were introduced at three of these sites in the mouse genome, support the conclusion that this mutant exerts a strong dominant negative effect on alternative DSB repair pathways (8). Notably, the most striking phenotype of this mouse was hematologic failure from replication stress; thus, the data presented here showing strong cellular phenotypes with agents that disrupt replication are consistent with DNA-PK binding DNA ends that result from replication stress. Here, using a mutational approach, we further characterize the mechanistic basis of the severe phenotype imparted by blocking phosphorylation of the ABCDE cluster in DNA-PKcs. We show that DNA-PK's catalytic activity is required for the dominant negative phenotype imparted by the ABCDE>Ala mutant and that phosphorylation of several other amino acids within DNA-PKcs is also necessary to elicit this phenotype. These data, coupled with emerging structural data, provide insight into how DNA-PK's autophosphorylation functions to regulate c-NHEJ.

MATERIALS AND METHODS

Expression plasmids. The expression constructs for wild-type (wt) DNA-PKcs, the K3753>R mutant, the ABCDE(T2609, S2612, T2620, S2624, T2638, T2647)>Ala mutant (where each residue is replaced with an alanine), and the ABCDE+PQR(S2023, S2029, S2041, S2053, S2056)+M(S3205)>Ala (with alanine substitutions at the PQR and M sites indicated) mutant have been previously described (9, 22, 23). To generate the additional combination mutants, restriction fragments from the K3753>R expression plasmid (PmlI-XmaI), the M(S3205)>Ala plasmid (11) (FseI-PmlI) the JK(T946, S1004)>Ala expression plasmid (11) (NarI-NarI), the T(T3950)>Ala expression plasmid (17) (PmlI-XmaI), and the N(S56, S72)>Ala expression plasmid (11) (MluI-BstZ17I) were subcloned into the corresponding sites in the ABCDE>Ala expression plasmid. All mutations were confirmed by sequence analysis.

The ABCDE^{EXT}+FG>Ala mutant was generated by synthesizing a fragment spanning the AgeI (residue 7608) to the FseI (8160) site by multiplex PCR. This fragment included a total of 18 Ser/Thr>Ala substitutions at the following amino acids: ABCDE^{EXT} sites S2599, T2600, T2603, T2609, S2612, T2615, T2620, S2624, T2638, T2645, T2647, and T2649; FG sites S2655, T2671, S2672, S2674, S2675, and S2677. The SalI site in wild-type DNA-PKcs at residue 8000 was ablated in this fragment, and a new SalI site was introduced in front of AgeI. This fragment was subcloned into the DNA-PKcs expression vector using SalI and FseI. To generate the ABCDE^{EXT}>Ala and FG>Ala mutants, the fragment containing all 18 Ser/Thr>Ala mutations was restricted with PstI (residue 7948), and each combination was generated. To facilitate cloning, the ABCDE^{EXT}>Ala and FG>Ala mutants were constructed in a much smaller, low-copy-number expression plasmid utilizing the CAGG promoter; thus, independent wild-type, ABCDE>Ala, and vector cell strains were also generated using this expression construct.

Cell culture and cell strains. Cells were cultured in minimum essential medium alpha (Gibco) with 10% fetal calf serum, 100 U/ml penicillin, 100 μg/ml streptomycin, and 10 μg/ml ciprofloxacin (complete medium) and maintained at 37°C with 5% CO_2. Methods to derive V3 transfectants have been previously described (11). Briefly, the DNA-PKcs-deficient Chinese hamster ovary cell line used as the parental cell strain, designated V3-CFP, was cotransfected with the DNA-PKcs expression plasmid indicated in the figure legends, and the pSuper.puro plasmid, to confer puromycin resistance, using FuGENE 6 (Roche) according to the manufacturer's instructions. Independent, stable transfectants were selected and maintained in complete medium containing 10 μg/ml puromycin. At least two independently derived clones expressing each mutant were studied and are presented in Fig. 3 and 5 to 8. For clonogenic assays presented in Fig. 1, only one clone is presented to simplify the figure; however, at least two clones expressing each mutant were studied with completely analogous results.

Immunoblotting and DSB-induced nuclear mobilization. Unless otherwise indicated, whole-cell extracts were generated by resuspending cell pellets in solubilization buffer (50 mM HEPES [pH 7.5], 50 mM NaF, 5 mM $MnCl_2$, 0.1% Triton X-100, 3 mg/ml DNase I, with protease and phosphatase inhibitors) and incubation at 37°C for 5 min. DNA-PKcs protein levels were analyzed after electrophoresis on 5% SDS-polyacrylamide gels and transfer to polyvinylidene difluoride membranes. To detect total DNA-PKcs, a monoclonal antibody raised against DNA-PKcs (42-27; a generous gift of Tim Carter, St. Johns University, New York, NY) was used as the primary antibody. For detection of DNA-PKcs or γH2AX following cisplatin exposure, cells were treated with cisplatin and allowed various amounts of time to repair, as described below. DNA-PKcs or γH2AX protein levels were analyzed in whole-cell extracts by immunoblotting using a primary antibody that recognizes either DNA-PKcs or γH2AX (Millipore).

To visualize nuclear mobilization of DNA-PKcs in response to DSBs, V3 transfectant strains were treated (or not) with 2 mg/ml zeocin in the absence of serum and antibiotics for 1 h at 37°C with 5% CO_2. Cells were harvested immediately after treatment or after 24 h of culture in fresh medium. A Triton-insoluble nuclear fraction was isolated as previously described (24) and analyzed by immunoblotting using primary antibodies that recognize either DNA-PKcs phospho-S2056 (Abcam), lamin B (Santa Cruz), or γH2AX (Millipore).

Clonogenic survival assays. For cells treated with zeocin, camptothecin, HU, cisplatin, MMS, and vincristine, V3 transfectants were plated at cloning densities into complete medium containing the dosages of the appropriate agent indicated in the figures. For HU and camptothecin, 24 h after treatment the medium containing the damaging agent was removed, and cells were replenished with fresh culture medium. For UV exposure, cells were plated at cloning density in complete medium and allowed 5 h to attach. The cells were washed with phosphate-buffered saline (PBS) and then irradiated with the doses of 254-nm UV (UV_{254}) indicated in the figures. For all agents, after 7 days cell colonies were stained with 1% (wt/vol) crystal violet in ethanol, and colony numbers were assessed. Survival was plotted as percent survival compared to untreated cells.

VDJ recombination assays. Extrachromosomal VDJ recombination assays were performed utilizing a coding joint substrate (pJH290) and signal joint substrate (pJH201) as described previously (25). Briefly, V3 cells were plated into 60-mm-diameter dishes and transiently transfected with 1 μg of substrate, 6 μg of wild-type or a mutant form of DNA-PKcs

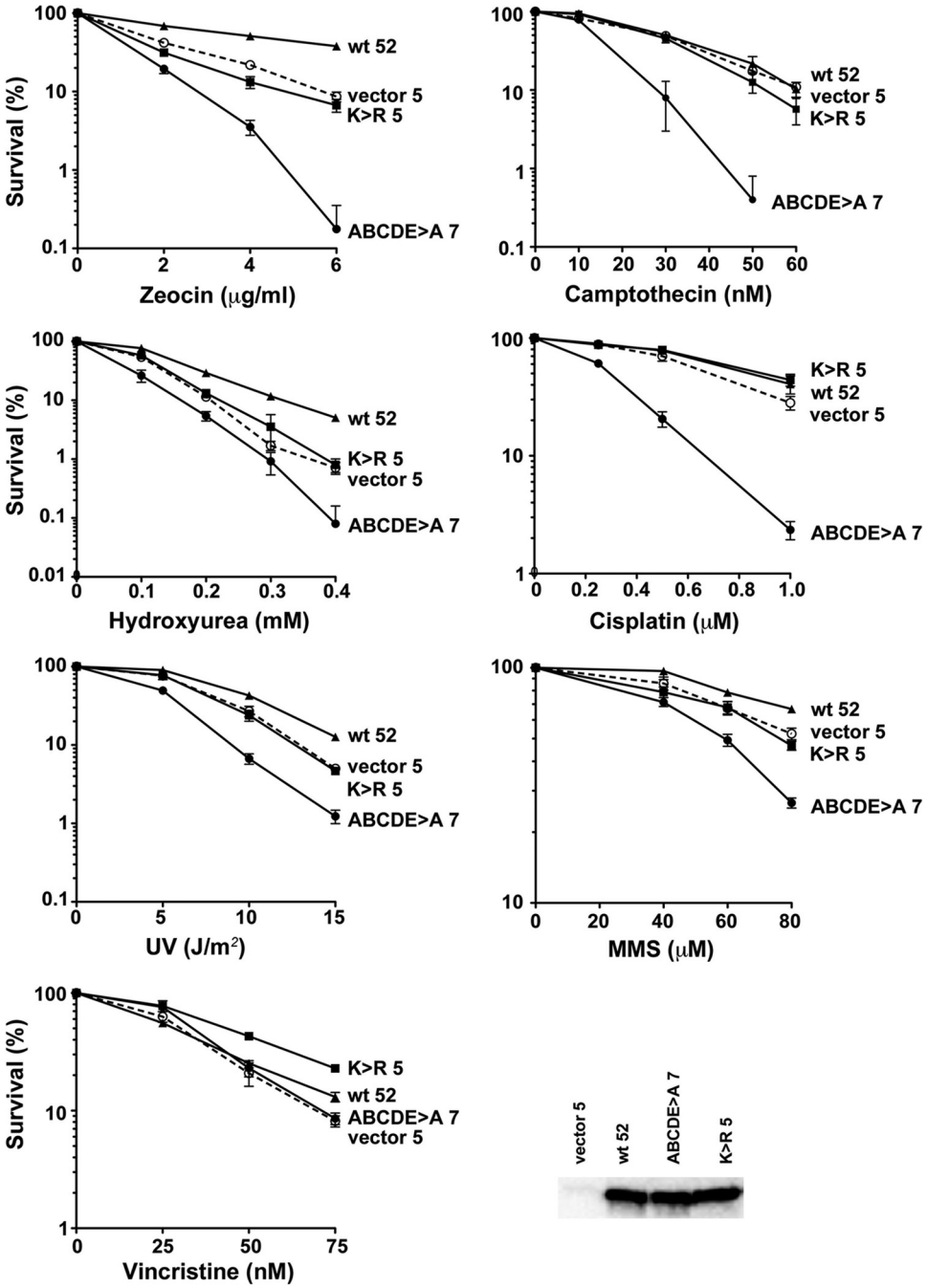

FIG 1 Blocking phosphorylation at the ABCDE sites sensitizes cells to many agents that damage DNA but not to an agent that disrupts microtubules. V3 transfectants expressing wild-type DNA-PKcs (wt strain 52), the catalytically inactive K3753>R mutant (K>R strain 5), the ABCDE>Ala cluster mutant (ABCDE>A strain 7), or no DNA-PKcs (vector strain 5) were plated at cloning densities into complete medium with increasing doses of the indicated DNA-damaging agent or the microtubule-destabilizing agent, vincristine. Colonies were stained after 7 days, and percent survival was calculated. Error bars represent the standard error of the means. Two independent cell strains were tested for each DNA-PKcs variant with similar results; one representative strain of each variant is presented here. DNA-PKcs protein expression levels of untreated cells were examined by Western blotting of whole-cell extracts obtained from the indicated cell strains (bottom, right).

or pCMV6 vector, and 2 μg each of RAG1 and RAG2 using FuGENE 6 transfection reagent. Forty-eight hours after transfection, substrate plasmids were isolated by alkaline lysis and subjected to DpnI digestion for 1 h. DpnI-digested DNA was transformed into competent DH5α cells (Invitrogen, Carlsbad, CA) according to the manufacturer's instructions. Transformed cells were spread onto LB agar plates containing 100 μg/ml ampicillin only or 100 μg/ml ampicillin and 22 μg/ml chloramphenicol. The percentage of recombination was calculated as the number of colonies resistant to ampicillin and chloramphenicol divided by the number of colonies resistant to ampicillin. Plasmid DNA from recombined pJH290 (coding joints) was isolated and sequenced at Michigan State University's core DNA sequencing facility.

Detection of cisplatin adducts in genomic DNA. Cells were plated at a density of 1×10^6 cells per well into six-well plates containing 2 ml of complete medium and allowed to grow for 24 h at 37°C with 5% CO_2. Cells were treated with 10 μM cisplatin, or no cisplatin, for 2 h at 37°C with 5% CO_2. After 2 h, the medium containing cisplatin was removed, and cells were washed with PBS and then replenished with fresh culture medium. Cells were allowed to repair for 0, 1, 2, 4, 24, and 48 h at 37°C with 5% CO_2. DNA was extracted from cells by lysis in the well and spooling as described by Laird et al. (26). DNA (30 to 50 μg) was hydrolyzed overnight in 1% nitric acid at 70°C in a 500-μl total volume. Samples were diluted to a 1.5-ml final volume in 1% nitric acid and analyzed by inductively coupled plasma-mass spectrometry (ICP-MS). A benchtop series Thermo ICPMS X-series II system with collision cell technology (CCT) capability and PlasmaLab software were used to quantify the platinum concentrations. The argon (Ar) plasma torch purity was at least 99.999% (Praxair Distribution, Inc.). Water was purified with a Milli-Q Advantage A10 System (Millipore). Optima nitric acid 67 to 70% (Fisher Scientific) was diluted to 2% and used as the solvent matrix while certified standard solutions were provided by Inorganic Ventures. ICP-MS calibration was conducted according to the manufacturer's specifications, followed by a multipoint curve fitted by linear regression with a minimum correlation coefficient (R^2) of 0.999.

Computational analyses of DNA-PKcs. Prediction of the secondary and tertiary structures was carried out using the PSIPRED (27) and HHpred (28) servers using the primary amino acid sequence of DNA-PKcs as the input query. Regions predicted as primarily disordered were assigned based on a lack of domain homology detection by HHpred and supported by a prediction of random coil by the PSIPRED server. Chain trajectory was estimated based on prior assignments of the N terminus, the HEAT repeats within the ring domain, and the kinase domain by Sibanda et al. (29).

RESULTS

Blocking DNA-PK's ABCDE phosphorylation hypersensitizes cells to many different DNA damaging agents. We showed previously that both hamster and mouse cells stably expressing human DNA-PKcs in which the ABCDE sites cannot be phosphorylated are hypersensitive to IR, mitomycin C, and etoposide (21). Recently DNA-PK has also been implicated in other repair processes (for instance, the response to replication stress) (30). We asked whether blocking ABCDE phosphorylation affected cell survival in the presence of additional agents that induce a variety of different types of DNA damage. As can be seen in Fig. 1, V3 clonal transfectants stably expressing the ABCDE>Ala mutant are more sensitive to camptothecin, HU, cisplatin, UV, MMS, and zeocin than V3 clonal transfectants expressing a catalytically inactive K3753>R variant of DNA-PKcs or no DNA-PKcs at all. All of these agents induce cell death by eliciting different types of DNA damage. We also tested cellular sensitivity to vincristine, which does not damage DNA but causes cell death by disrupting microtubules; all cell types are similarly sensitive to vincristine. We conclude that blocking ABCDE phosphorylation hypersensitizes cells to many DNA damaging agents that cause a variety of types of DNA lesions.

Blocking DNA-PK's ABCDE phosphorylation impairs removal of cisplatin adducts from DNA. We considered two possibilities to explain why blocking ABCDE phosphorylations hypersensitizes cells to DNA damage: (i) the ABCDE>Ala mutant blocks access to DNA ends (that are generated during repair of a variety of different lesions) by other repair pathways (HR or a-NHEJ), or (ii) the ABCDE>Ala mutant induces cell death by inappropriate signaling. We reasoned that if the ABCDE>Ala mutant blocked repair by other pathways, DNA damage should be retained longer. Unlike damage induced by irradiation, some DNA damaging agents generate covalent adducts in DNA that can be measured by physical means. Cisplatin adducts are readily measured by mass spectrometry (ICP-MS methodology). To address whether DNA damage was retained longer in cells expressing the ABCDE>Ala mutant, removal of adducts from the DNA of cells treated with cisplatin was measured. Removal of cisplatin adducts in cells expressing the ABCDE>Ala mutant was delayed by approximately 24 h (Fig. 2A). Longer persistence of cisplatin adducts would be consistent with the ABCDE>Ala mutant blocking access of DNA ends to other repair pathways (as opposed to inducing inappropriate signaling). It should be noted that cells expressing wild-type DNA-PKcs removed cisplatin-DNA adducts just slightly more slowly than cells expressing no DNA-PKcs. This is consistent with studies showing that DNA-PKcs-deficient cells often display reduced sensitivity to cross-linking agents (21, 31); this is observed in V3 transfectants at higher doses of cisplatin, and the increased sensitivity is dependent on DNA-PKcs expression levels (K. Meek, unpublished data).

Repair of interstrand DNA cross-links involves incisions on either side of the cross-link ("unhooking") by nucleotide excision repair (NER) followed by translesion synthesis and/or recombinational repair. The ability of DNA-PK to oppose HR is well appreciated (11), and since HR is initiated by DSBs, it seems that the HR pathway may be the most likely impacted by ABCDE>Ala during repair of cisplatin-induced damage. We considered that the increased cisplatin sensitivity might also result in increased accumulation of DSBs (because the repair of DSBs is blocked by the presence of ABCDE>Ala); γH2AX levels were measured as an indicator of persistent DSBs. Whereas cells lacking DNA-PKcs have only a minimal increase in γH2AX after cisplatin damage (consistent with rapid removal of the lesions), cells expressing wild-type DNA-PKcs have a more pronounced, but transient, increase in γH2AX. In contrast, the levels of γH2AX in cisplatin-treated cells expressing the ABCDE>Ala mutant are higher and more sustained than in cells expressing wild-type DNA-PKcs or no DNA-PKcs, consistent with the presence of unrepaired DSBs (Fig. 2B). DNA-PKcs itself is actually a well-studied target of caspase 3 and the apoptotic cascade (32, 33). Thus, DNA-PKcs levels were measured (as an indirect measure of apoptosis) in cells expressing wild-type DNA-PKcs or the ABCDE>Ala mutant for 48 h after cisplatin exposure. As can be seen, DNA-PKcs levels are not changed, and no evidence of DNA-PKcs cleavage is observed (Fig. 2C). These data suggest that the ABCDE>Ala mutant exerts its dominant negative effect, at least with respect to repair of cisplatin adducts, by blocking access of the HR pathway to DNA ends.

Enzymatic activity is required for the ABCDE dominant negative effect. In an effort to understand the molecular basis of the ABCDE dominant negative effect, we first determined whether DNA-PK's catalytic activity is required for its ability to block DNA end access to other repair factors. To that end, a mutant was generated and characterized that combined the ABCDE>Ala and the kinase-inactivating K3753>R mutations (Fig. 3); two independent V3 clones stably expressing each construct were isolated and studied. Whereas wild-type DNA-PKcs reverses the zeocin-sensitive phenotype of V3 cells, the ABCDE>Ala mutant dramatically worsens this phenotype. In contrast, zeocin sensitivity of the combined mutations, ABCDE>Ala+K3753>R, is analogous to that of cells that completely lack DNA-PKcs, indicating that DNA-

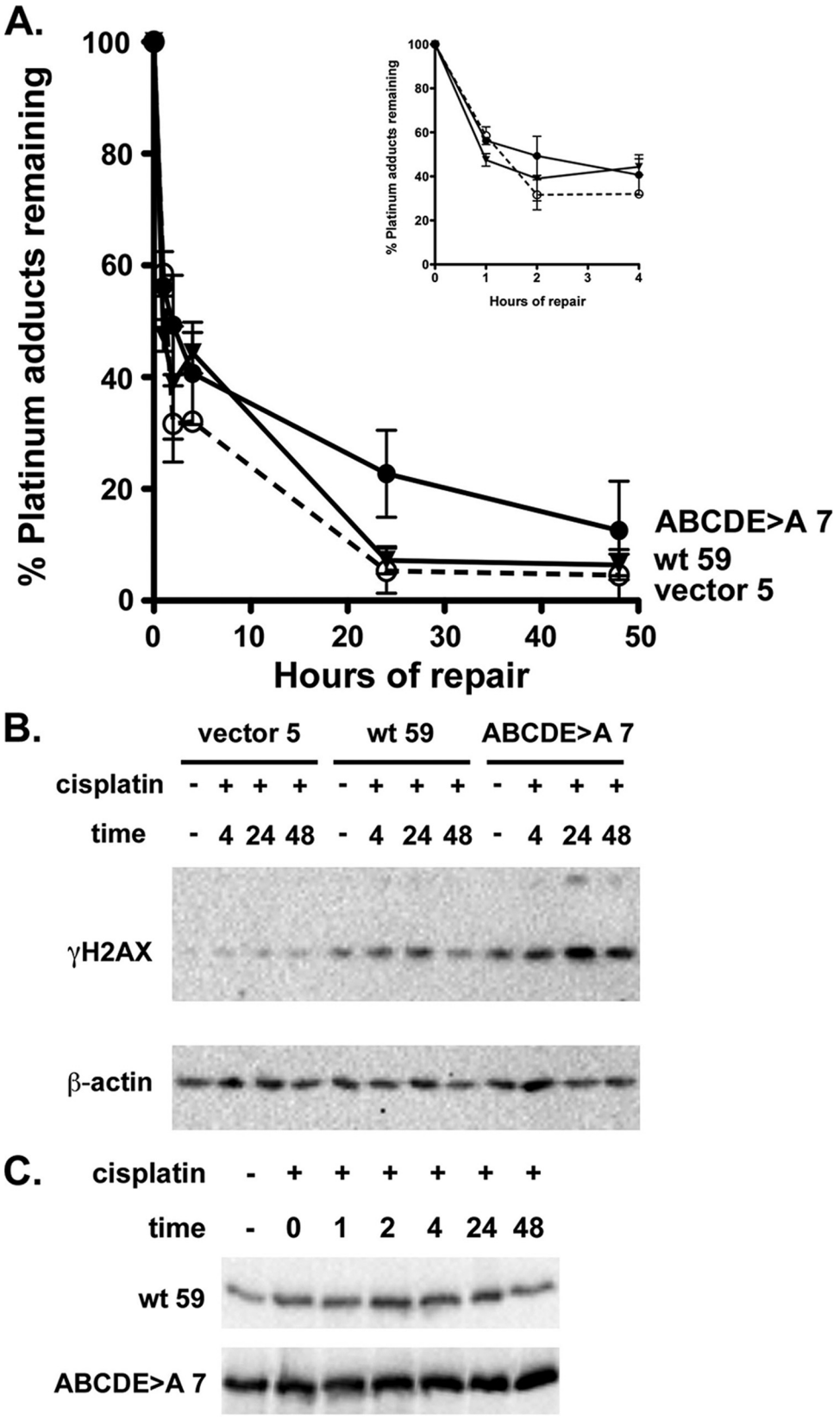

FIG 2 Blocking phosphorylation at the ABCDE sites decreases the rate at which cells remove cisplatin. (A) V3 transfectants expressing wild-type DNA-PKcs (wt strain 59), the ABCDE>Ala mutant (strain 7), or no DNA-PKcs (vector strain 5) were treated with 10 μM cisplatin for 2 h and then allowed 0, 1, 2, 4, 24, or 48 h to repair. The percentage of platinum adducts remaining in the genomic DNA was then analyzed by ICP-mass spectrometry. The inset shows an expanded view of the 0-, 1-, 2-, and 4-h time points. Error bars represent the standard errors of the means. (B) V3 transfectants expressing

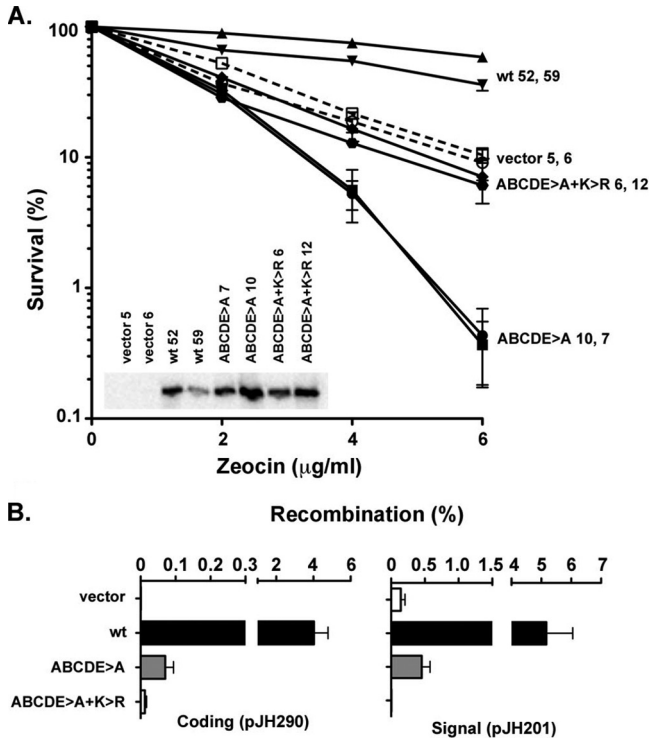

FIG 3 Enzymatic activity is required for the ABCDE>Ala phenotype. (A) Two independent V3 transfectant cell strains expressing wild-type DNA-PKcs (wt strains 52 and 59), the ABCDE>Ala mutant (strains 7 and 10), the ABCDE>Ala+K3753>R combination mutant (strains 6 and 12), or no DNA-PKcs (vector strains 5 and 6) were plated at cloning densities into complete medium containing increasing doses of zeocin as indicated. Colonies were stained after 7 days, and percent survival was calculated. Error bars represent standard error of the means. The inset shows the level of DNA-PKcs protein expression in untreated cells as determined by Western blotting of whole-cell extracts obtained from the indicated cell strains. (B) Recombination percentage of the coding joint substrate pJH290 or signal joint substrate pJH201 in V3 cells transiently expressing RAG proteins and either wild-type DNA-PKcs, the ABCDE>Ala mutant, the ABCDE>Ala +K375>R combination mutant, or no DNA-PKcs. Error bars represent the standard error of the means. Note that the differences between the recombination efficiencies of the ABCDE>Ala and the ABCDE>Ala +K3753>R mutants for both coding end joining ($P \leq 0.05$) and signal end joining ($P \leq 0.01$) are statistically significant based on a two-tailed unpaired *t* test.

PK's enzymatic activity is required for the ABCDE>Ala dominant negative phenotype.

Each mutant was also tested for its ability to complement the VDJ recombination defects associated with DNA-PKcs deficiency utilizing an episomal assay developed by Hesse and colleagues (25). Although cells expressing the ABCDE>Ala mutant are remarkably more sensitive to zeocin than cells expressing no DNA-PKcs, both VDJ coding and signal end joining are consistently increased in cells expressing the ABCDE>Ala mutant compared to cells that lack DNA-PKcs (9) (Fig. 3B); this may seem counterintuitive. However, whereas clonogenic survival indirectly measures the cells' capacity to repair DSBs induced by zeocin using all DSB repair pathways (HR, a-NHEJ, and c-NHEJ), repair of VDJ recombination intermediates can only be mediated by c-NHEJ. This is because recombination-activating gene (RAG)-induced breaks, i.e., VDJ recombination intermediates, are blocked from a-NHEJ although the mechanisms are poorly understood (4, 34). Thus, the low levels of VDJ joining indicate that cells expressing the ABCDE>Ala mutant can execute a minimal level of c-NHEJ. We suggest that the ABCDE>Ala mutant initiates c-NHEJ, forming a functional c-NHEJ complex, but progress of repair is impaired perhaps because ABCDE phosphorylation is required to initiate end processing. The impaired c-NHEJ mediated by the ABCDE>Ala mutant might also block access of the DSB to other repair pathways (HR or perhaps a-NHEJ), resulting in hypersensitivity to zeocin of cells expressing this mutant.

Evidence that ABCDE is present in an unstructured region. Implicit in the finding that kinase activity is required for the ABCDE dominant negative effect is that another phosphorylation event or events are required to inhibit access of DNA ends to other repair pathways. Our previous studies have shown that, in many cases, phosphorylations of DNA-PKcs itself are functionally relevant; thus we next focused on determining whether other DNA-PKcs phosphorylations are required for the ABCDE dominant negative effect. To facilitate interpretation of these data, it is helpful to understand relative positions of the phosphorylation sites within the DNA-PK complex. Figure 4A depicts the phosphorylation sites studied previously and summarizes phenotypes associated with each phosphorylation site mutant using both cellular and biochemical assays (9–11, 14, 15, 17, 18, 21, 22, 35, 36). Table S1 in the supplemental material also defines every phosphorylation site studied.

Structure/function studies of the DNA-PK complex have been hampered by a lack of high-resolution structural information. A low-resolution crystal structure at 6.6 Å of DNA-PKcs has been reported (29). The resolution of the structure allows only a rough estimation of the overall shape of the molecule. Importantly, this low-resolution crystal structure shares many features with previous cryo-electron microscopy (cryo-EM) structures of DNA-PK (37–40) and with solution structures recently reported using small-angle X-ray scattering (SAXS) techniques (5, 41).

The modeled structure includes seven distinct regions (29) (Fig. 4B). The phosphatidylinositol 3-kinase (PI3K) domain is shown in yellow and is positioned in the domain termed the head domain in cryo-EM studies. The FAT and FATC domains are magenta. The ring-shaped structures (shown in green) derive from the N terminus (also referred to as the palm domain in previous studies). The ring structure is comprised entirely of HEAT repeats and has a gap at the base. The authors speculated that DNA is threaded through the gap at the base of the ring. The ring is concave (or cradle shaped) when viewed from the side. Sibanda et al. proposed a DNA binding pocket (cyan).

We performed secondary-structure analysis using PSIPRED (27) and searched for domain homologies using HHpred (28).

wild-type DNA-PKcs, the ABCDE>Ala mutant, or no DNA-PKcs (vector) were treated with 10 μM cisplatin for 2 h and then allowed 4, 24, or 48 h to repair. Whole-cell extracts were analyzed by Western blotting for the level of γH2AX expression. The level of β-actin expression was used as a loading control. One of three independent experiments performed with identical results is depicted. (C) V3 transfectants expressing wild-type DNA-PKcs or the ABCDE>Ala mutant were treated with 10 μM cisplatin for 2 h and then allowed 0, 1, 2, 4, 24, or 48 h to repair. Whole-cell extracts were analyzed by Western blotting for the level of DNA-PKcs expression. One of two independent experiments performed with identical results is depicted.

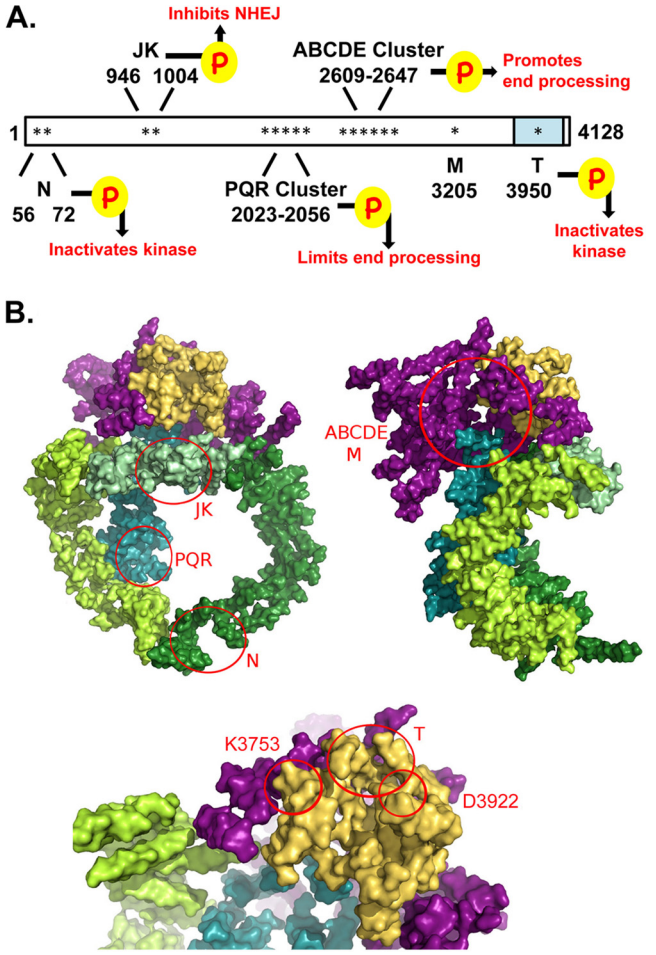

FIG 4 Current Model of DNA-PKcs. (A) Schematic of DNA-PKcs polypeptide showing the position of previously studied phosphorylation (P) sites; the kinase domain is shaded blue, and phosphorylation sites are denoted by asterisks (N, S56 and S72; JK, T946 and S1004; PQR, S2023, S2029, S2041, S2053, and S2056; ABCDE, T2609, S2612, T2620, S2624, T2638, and T2647; M, S3205). (B) Molecular surface of DNA-PKcs (29) showing seven regions of the DNA-PKcs polypeptide including an approximation of the positions of the phosphorylation sites and catalytic site (K3753) studied here, as determined by PSIPRED analysis.

With this information, we attempted to trace the primary amino acid sequence onto the structure and to assign the seven regions including 2,032 residues to specific regions in DNA-PKcs. Sibanda et al. assigned the N terminus to the gap at the base of the ring domain. The polypeptide can be traced from the base of the ring, counterclockwise, toward the forehead or brow. Then, the most likely trajectory is for the chain to continue counterclockwise down toward the base of the ring. Upon reaching the gap formed with the N terminus, the protein appears to reverse its trajectory, moving up toward the FAT domain. The trace ends at the kinase domain. An estimation of the location of the sites studied here is shown in Fig. 4B: N sites are at the N-terminal base of the ring domain, JK sitesare in the ring domain, the PQR cluster is in the ring domain, perhaps close to the putative DNA binding pocket, the M site is in the FAT domain, the T site is in the PI3K domain, and the catalytic K3753 and D3922 residues are in the PI3K domain. Importantly, the ABCDE sites cannot be positioned in any of these chains. PSIPRED returns its secondary-structure predictions with a score between 0 and 9, reflecting the confidence of the prediction. The region encompassing residues 2500 to 2700 including the ABCDE phosphorylation cluster is predicted to be entirely disordered with only one short sequence predicted to be helical (6 residues), and that prediction is with low confidence (scores of 0 to 3). In sum, the PSIPRED analysis indicated a greater than 75% likelihood for lack of secondary structure in this region. Moreover, HHpred searches of this region with existing protein structures yielded no significant matches for secondary structure.

Intrinsically disordered segments in proteins are often regions found to be critical for important biologic functions (42). Although the ABCDE cluster is in a region absent in the crystal structure, from modeling regions adjacent in the primary sequence, it can be assumed that the ABCDE cluster is likely to be located at a hinge-like region between the head domain (FAT/kinase/FATC) and the large ring domain. Dobbs et al. also suggested that the ABCDE phosphorylation sites are in this region (5). Although the placement of these phosphorylation targets is only an estimation, we reasoned that having even a rough estimation of the spatial positions of different phosphorylation targets might facilitate data interpretation. It is interesting that similar computational analyses with ATR and ATM did not predict any extensive areas of random coil in either polypeptide compared to DNA-PKcs.

To address if (and which) additional phosphorylations might be required for the dominant negative phenotype of the ABCDE>Ala mutant, alanine blocking mutations of 11 previously studied DNA-PKcs phosphorylation sites (depicted in Fig. 4A and listed in Table S1 in the supplemental material) were introduced into the expression construct encoding the ABCDE>Ala mutant and characterized functionally. All of these alanine mutants, as well as all combination mutants studied below, retained full enzymatic activity (see Fig. S1 in the supplemental material). Since these assays require DNA-PKcs assembly onto Ku-bound DNA, enzymatic activity strongly suggests that the mutants can assemble onto Ku-bound DNA. To confirm that the enzymatic activity is dependent on Ku–DNA-PKcs interactions, enzymatic activity was also assessed in an xrs6 cell transfectant (which lacks Ku86) expressing human DNA-PKcs. As expected, even though high levels of DNA-PKcs are expressed, in the absence of Ku, no enzymatic activity was detected (see Fig. S1).

Blocking phosphorylation of S3205 (an ATM target) does not alter the ABCDE>Ala phenotype. We have previously defined S3205, referred to as site M, as an *in vitro* DNA-PK autophosphorylation site (36) and studied this site in conjunction with the ABCDE, PQR, and T3950 sites, but not with ABCDE>Ala substitutions alone. This S/hydrophobic site is strongly conserved in vertebrate DNA-PKcs and has been identified as an *in vivo* phosphorylation site in numerous genome-wide phosphoproteomics screens (reviewed in reference 5). More recently, S3205 was identified as an IR-induced phosphorylation site in a genome-wide analysis of sites phosphorylated in the DNA damage response (43) and as an ATM target in response to DNA damage (44). As can be seen in Fig. 5, two independent clones expressing the combined ABCDE+M>Ala mutant behave indistinguishably from ABCDE>Ala transfectants in zeocin clonogenic survival assays and VDJ recombination assays. Moreover, sequence analysis of coding joints in cells expressing ABCDE+M>Ala show severely restricted end processing, analogous to joints mediated by the

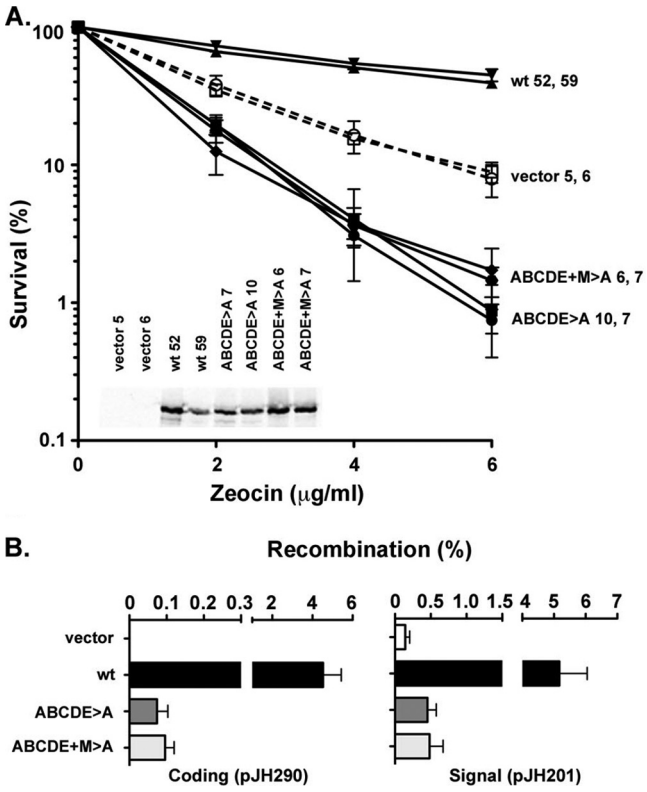

FIG 5 Blocking phosphorylation of the M site does not alter the ABCDE phenotype. (A) Two independent V3 transfectant cell strains expressing wild type DNA-PKcs (wt strains 52 and 59), the ABCDE>Ala mutant (strains 7 and 10), the ABCDE+M>Ala combination mutant (strains 6 and 7)), or no DNA-PKcs (vector strains 5 and 6) were plated at cloning densities into complete medium containing increasing doses of zeocin as indicated. Colonies were stained after 7 days, and percent survival was calculated. Error bars represent the standard error of the means. The inset shows the level of DNA-PKcs protein expression in untreated cells as determined by Western blotting of whole-cell extracts obtained from the indicated cell strains. (B) Recombination percentage of the coding joint substrate pJH290 or signal joint substrate pJH201 in V3 cells transiently expressing RAG proteins and either wild-type DNA-PKcs, the ABCDE>Ala mutant, the ABCDE+M>Ala combination mutant, or no DNA-PKcs. Error bars represent the standard error of the means. Note that the differences between the recombination efficiencies of the ABCDE>Ala and the ABCDE+M>Ala mutants for both coding end joining ($P > 0.05$) and signal end joining ($P > 0.05$) are not statistically significant based on a two-tailed unpaired *t* test.

ABCDE>Ala mutant (Table 1). We conclude that phosphorylation of S3205 does not affect the phenotype imparted by expressing the ABCDE>Ala mutant.

Phosphorylation of sites potentially adjacent to the DNA binding pocket is required for the ABCDE>Ala dominant negative phenotype. In the proposed structural model, when the kinase is viewed from the side (Fig. 4B), one can appreciate that the PQR/JK and ABCDE sites may be adjacent to the region where the head and ring domains intersect (with the PQR sites being positioned in the putative DNA binding pocket and the JK sites just above). It is worth noting that our previous studies (10) have shown that phosphomimicking the PQR sites results in severe restriction of end processing while maintaining robust NHEJ capacity. This is conceptually consistent with a model whereby PQR phosphorylation promotes DNA end binding and limits end access to other factors. We have previously partially characterized a combined ABCDE+PQR+M>Ala mutant (10). As can be seen, cells expressing the combined ABCDE+PQR+M>Ala or the ABCDE+JK>Ala mutant are more resistant to zeocin than cells expressing the ABCDE>Ala mutant (Fig. 6). In contrast, the minimal coding end and signal end joining of the ABCDE>Ala mutant is completely ablated by blocking PQR phosphorylation; coding end joining (but not signal end joining) is also partially abrogated by blocking JK phosphorylation. Sequence analysis of rare coding joints in cells expressing ABCDE+PQR+M>Ala show that the severe restriction of end processing imparted by the ABCDE>Ala mutant is reversed by blocking PQR phosphorylation (Table 1). This is consistent with our previous characterization of the PQR>Ala mutant, which allows extensive end processing. The severe restriction of end processing by blocking ABCDE phosphorylation is also reversed in the ABCDE+JK>Ala mutant; however, in this case end processing levels are returned to wild-type levels. The JK>Ala mutant does not affect end processing on its own, but phospho-mimicking these sites strongly impedes c-NHEJ (11). Although other explanations are possible, the differences in VDJ recombination efficiency between ABCDE+PQR+M>Ala and ABCDE+JK>Ala may be a reflection of the dependence on PQR phosphorylation for efficient c-NHEJ versus JK phosphorylation, which inhibits c-NHEJ (11). Experiments investigating the basis for these differences are ongoing. However, we interpret this reduction in VDJ joining for both of these combined mutants as evidence of reduced c-NHEJ. We suggest that the reduced c-NHEJ (by blocking PQR and JK phosphorylation) may allow increased

TABLE 1 Characterization of coding joints mediated by DNA-PKcs mutants

DNA-PKcs	No. of sequences	Avg no. of bases lost/joint	Median no. of bases lost/joint	% complete ends[a]	% short sequence homology[b]	% P segments[c]
Wild type	43	4.95	4	34 (29/86)	44 (19/43)	14 (4/29)
ABCDE>Ala	37	2.97	1.0	62 (46/74)	11 (4/37)	11 (5/46)
ABCDE>Ala +K3753>R	12	37.42	12.5	17 (4/24)	50 (6/12)	75 (3/4)
ABCDE+M>Ala	38	1.18	1.0	68 (52/76)	5 (2/38)	31 (16/52)
ABCDE+PQR+M>Ala	33	20.91	8	30 (20/66)	39 (13/33)	50 (10/20)
ABCDE+JK>Ala	36	4.78	3.0	49 (35/72)	22 (18/36)	31 (11/35)
ABCDE+N>Ala	42	2.36	1.5	60 (50/84)	17 (7/42)	36 (18/50)
ABCDE+T>Ala	33	8.15	4	44 (29/66)	39 (13/33)	31 (9/29)
ABCDE+PQR+M+T>Ala	8	16.13	7.5	50 (8/16)	25 (2/8)	75 (6/8)

[a] Values in parentheses represent the number of intact coding ends/total number of ends.
[b] Values in parentheses represent the number of sequences with short sequence homology/total number of sequences.
[c] Values in parentheses represent the number of P segments/number of complete ends.

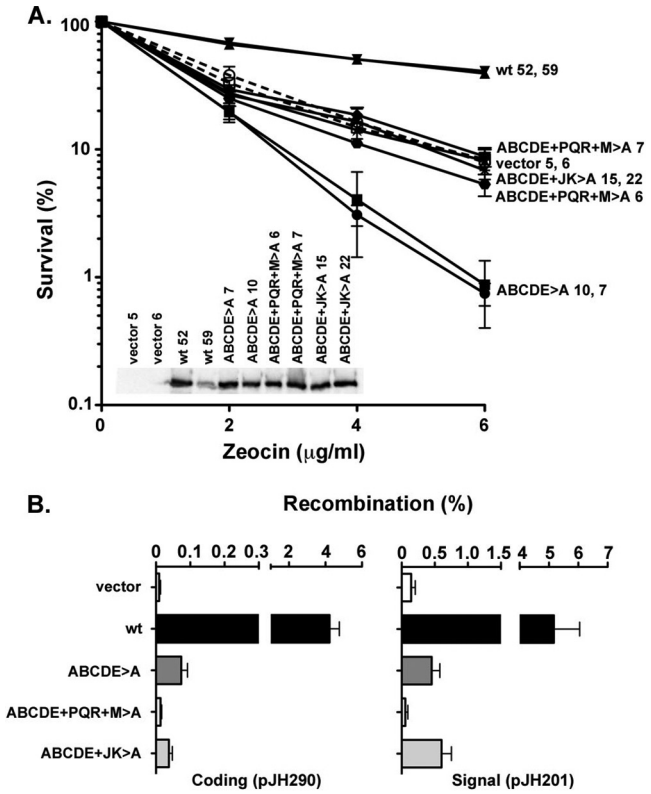

FIG 6 Phosphorylation of the PQR and JK sites, which are predicted to be near the putative DNA binding pocket, is required for the ABCDE phenotype. (A) Two independent V3 transfectant cell strains expressing wild-type DNA-PKcs (wt strains 52 and 59), the ABCDE>Ala mutant (strains 7 and 10), the ABCDE+PQR+M>Ala combination mutant (strains 6 and 7), the ABCDE+JK>Ala combination mutant (strains 15 and 22), or no DNA-PKcs (vector strains 5 and 6) were plated at cloning densities into complete medium containing increasing doses of zeocin as indicated. Colonies were stained after 7 days, and percent survival was calculated. Error bars represent standard error of the means. The inset shows the level of DNA-PKcs protein expression in untreated cells as determined by Western blotting of whole-cell extracts obtained from the indicated cell strains. (B) Recombination percentage of the coding joint substrate pJH290 or signal joint substrate pJH201 in V3 cells transiently expressing RAG proteins and either wild-type DNA-PKcs, the ABCDE>Ala mutant, the ABCDE+PQR+M>Ala combination mutant, the ABCDE+JK>Ala combination mutant, or no DNA-PKcs. Error bars represent the standard error of the means. Note that the differences between the recombination efficiencies of the ABCDE>Ala and the ABCDE+PQR+M>Ala mutants for both coding end joining ($P \leq 0.01$) and signal end joining ($P \leq 0.01$) are statistically significant based on a two-tailed unpaired t test. The difference between the coding end joining efficiency of the ABCDE>Ala and the ABCDE+JK>Ala mutants is statistically significant ($P \leq 0.05$). However, the difference between the signal end joining efficiencies of these mutants is not significant ($P > 0.05$).

access of DNA ends to a-NHEJ and presumably HR, resulting in increased survival after zeocin exposure. In any case, we conclude that phosphorylations of the PQR and JK sites facilitate the dominant negative phenotype of the ABCDE>Ala mutant. We speculate that, since structural modeling (Fig. 4B) suggests that both JK and PQR sites may be close to the DNA binding pocket, JK and PQR phosphorylations may facilitate positioning and/or maintenance of the DNA ends into the DNA-PKcs DNA binding pocket, restricting access to DNA ends from other repair factors. We suggest that PQR and JK phosphorylations (at least in the absence of ABCDE phosphorylation) impede phosphorylation-induced dissociation of DNA-PKcs from Ku-bound DNA.

Phosphorylation of sites that result in kinase inactivation facilitates the ABCDE>Ala dominant negative phenotype. Although phosphorylation in the activation or "t" loop of most protein kinases induces enzymatic activity, our previous studies suggest that phosphorylation within DNA-PKcs's t-loop (T3950, T site) inactivates the enzyme. More recently, we have also shown that phosphorylation of the N sites (S56 and S72), which are highly conserved S-hydrophobic sites at the extreme N terminus, partially inactivates the enzyme. However, it is unlikely that either N or T phosphorylation results in DNA-PKcs dissociation from Ku-bound DNA (11, 17). Thus, DNA-PK can self-inactivate by multiple mechanisms: (i) phosphorylation of T, (ii) phosphorylation of N, or (iii) phosphorylation-induced kinase dissociation. Presumably, a DNA-PKcs molecule inactivated by T or N phosphorylation could still dissociate by trans-autophosphorylation of a synapsed complex.

We next tested the effect of blocking kinase inactivation on the ABCDE dominant negative phenotype. As can be seen in Fig. 7, cells expressing either the combined ABCDE+T>Ala or ABCDE+N>Ala mutant are more resistant to zeocin than cells expressing the ABCDE>Ala mutant. (Three independent ABCDE+N>Ala clones were tested because cells expressing ABCDE+N>Ala are slightly more zeocin resistant than cells lacking DNA-PKcs; this difference was only notable for one of the three clones studied.) Minimal coding and signal end joining mediated by the ABCDE>Ala mutant are completely ablated by blocking T but not N phosphorylation. Sequence analysis of rare coding joints in cells expressing ABCDE+T>Ala shows that blocking T but not N phosphorylation reverses the severe restriction of end processing imparted by the ABCDE>Ala mutant (Table 1). We are further investigating the basis for these differences in VDJ recombination phenotypes. However, we can conclude that T and N phosphorylations facilitate the dominant negative phenotype of the ABCDE>Ala mutant.

One possible explanation for these data is that when autophosphorylation-induced dissociation is slowed, as is the case when ABCDE phosphorylation is blocked, kinase inactivation (by T or N phosphorylation) facilitates prolonged DNA-PK occupancy at a DSB. It follows that blocking either T or N phosphorylation might maintain enzymatic activity, allowing phosphorylation of sites that contribute to complex dissociation that normally works in conjunction with phosphorylation of ABCDE, thus abrogating ABCDE's dominant negative effect.

Phosphorylations adjacent to the ABCDE cluster contribute to its function. Although the first biochemical feature attributed to DNA-PK's autophosphorylation was kinase dissociation (discovered almost 20 years ago) (45), the mechanistic basis for this process has not been clarified. We have shown previously using two distinct biochemical approaches (9, 17) that although the ABCDE>Ala mutant can undergo phosphorylation-dependent dissociation from Ku-bound DNA, the ABCDE>Ala mutant dissociates somewhat more slowly than wild-type DNA-PKcs, thus implicating ABCDE phosphorylation in kinase disassembly. However, this effect is completely abrogated by blocking PQR phosphorylations (17). Dobbs et al. reviewed recent proteomic phosphorylation studies of DNA-PKcs (5); several independent studies have shown that 12 additional serine or threonine residues adjacent to the ABCDE cluster are phosphorylated in living cells in

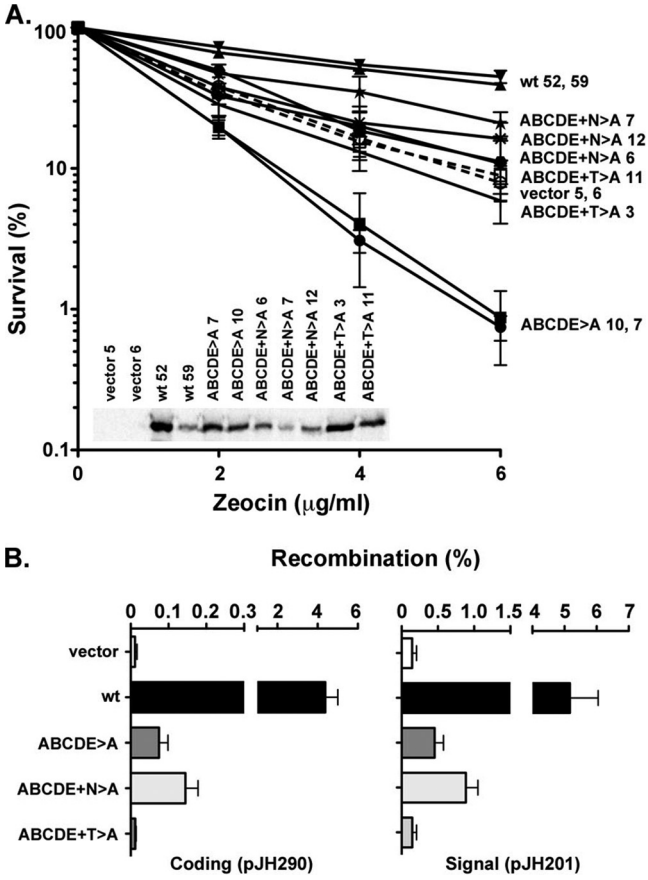

FIG 7 Phosphorylation of the N and T sites, which regulate enzymatic activity, is required for the ABCDE phenotype. (A) Two or three independent V3 transfectant cell strains expressing wild-type DNA-PKcs (wt strains 52 and 59), the ABCDE>Ala mutant (strains 7 and 10), the ABCDE+N>Ala combination mutant (strains 6, 7, and 12), the ABCDE+T>Ala combination mutant (strains 3 and 11), or no DNA-PKcs (vector strains 5 and 6) were plated at cloning densities into complete medium containing increasing doses of zeocin as indicated. Colonies were stained after 7 days, and percent survival was calculated. Error bars represent standard error of the means. The inset shows the level of DNA-PKcs protein expression in untreated cells as determined by Western blotting of whole-cell extracts obtained from the indicated cell strains. (B) Recombination percentage of the coding joint substrate pJH290 or signal joint substrate pJH201 in V3 cells transiently expressing RAG proteins and either wild-type DNA-PKcs, the ABCDE>Ala mutant, the ABCDE+N>Ala combination mutant, the ABCDE+T>Ala combination mutant, or no DNA-PKcs. Error bars represent the standard error of the means. Note that the differences between the recombination efficiencies of the ABCDE>Ala and the ABCDE+N>Ala mutants for both coding joining ($P > 0.05$) and signal end joining ($P > 0.01$) are not statistically significant based on a two-tailed unpaired t test. However, the differences between the recombination efficiencies of the ABCDE>Ala and the ABCDE+T>Ala mutants for both coding end joining ($P \leq 0.01$) and signal end joining ($P \leq 0.05$) are statistically significant.

response to a variety of different genotoxic stressors (5, 6). These 12 additional sites are well conserved and are located within 78 residues (spanning residues 2599 to 2677) included in the region predicted by PSIPRED to lack secondary structure. We considered that ABCDE phosphorylation is responsible for kinase dissociation but that this cluster actually includes additional secondary sites that can facilitate dissociation if the primary sites cannot be phosphorylated (because of alanine substitution). Six of these sites (residues 2599, 2600, 2603, 2615, 2645, and 2649) are within or just N terminal of the ABCDE cluster. The other six sites (residues 2655, 2671, 2672, 2674, 2675, and 2677) are slightly C terminal. Three additional constructs were generated: (i) ABCDE^{EXT}>Ala introduces alanine substitutions at 12 sites (including the six previously characterized ABCDE sites) between residues 2599 and 2649; (ii) FG introduces substitutions at six sites between residues 2655 to 2677; (iii) ABCDE^{EXT}+FG>Ala introduces substitutions at all 18 sites in this region (Fig. 8A; see also Fig. S2A and S3A in the supplemental material).

We first focused on the ABCDE^{EXT}>Ala construct that blocks the additional six sites within and slightly N terminal to the ABCDE cluster; four of these six sites are S-T/hydrophobic sites, potentially preferred DNA-PK targets. These new constructs were generated using a different expression vector; thus, new wild-type, ABCDE>Ala, and vector clones stably expressing DNA-PKcs were generated and used in these experiments. As can be seen in Fig. 8, cells expressing the ABCDE^{EXT}>Ala mutant are similarly sensitive to zeocin as cells expressing the ABCDE>Ala mutant. However, the minimal coding end joining mediated by the ABCDE>Ala mutant is completely ablated by blocking all 12 sites. This is the only phosphoblocking DNA-PKcs mutant that imparts a strong dominant negative effect in zeocin clonogenic assays and ablates the minimal coding and signal VDJ joining activity observed in cells expressing the ABCDE>Ala mutant. Coding end joining was so severely reduced (less than 0.4% of wild-type levels) that only four joints were isolated in 24 independent assays (data not shown). These data are consistent with the idea that the additional six sites can function as back-up sites (if the primary sites cannot be phosphorylated because of alanine substitution), facilitating the minimal c-NHEJ observed in cells expressing the ABCDE>Ala mutant.

Elegant studies from Drouet and colleagues have shown that c-NHEJ factors mobilize to a Triton-insoluble fraction after DNA damage, presumably reflecting their association with DNA damage during repair (24). We have utilized this assay previously and found that the ABCDE>Ala mutant is maintained in this Triton-insoluble fraction longer than wild-type DNA-PKcs. We performed a similar analysis with cells expressing wild-type, ABCDE>Ala, and ABCDE^{EXT}>Ala mutant DNA-PKcs. As can be seen in Fig. 8D, although wild-type DNA-PKcs is detected in this fraction immediately after zeocin induced damage, it is absent from this fraction 24 h after damage. In contrast, both the ABCDE>Ala and ABCDE^{EXT}>Ala mutants are present in this fraction 24 h postexposure to zeocin. Additional biochemical approaches will be required to assess whether the ABCDE^{EXT}>Ala mutant has a more complete obstruction in autophosphorylation-induced complex dissociation than the ABCDE>Ala mutant.

We next tested the effect of blocking the additional six (FG) sites just C terminal of the ABCDE cluster. It has been reported that these sites are phosphorylated in living cells in response to a variety of genotoxic stressors. But unlike the sites within ABCDE, these sites have also been reported to be phosphorylated during mitosis (46, 47). None of these sites are S-T/Q target sites, and only one is S-T/hydrophobic. We tested the effect of blocking FG phosphorylation, with and without ABCDE^{EXT} ablation. Cells expressing the FG>Ala mutant are indistinguishable from cells expressing wild type DNA-PKcs in both zeocin survival assays and VDJ recombination assays (see Fig. S2 in the supplemental material). However, blocking FG phosphorylation reverses the zeocin hypersensitivity observed by blocking the ABCDE^{EXT}>Ala sites (see

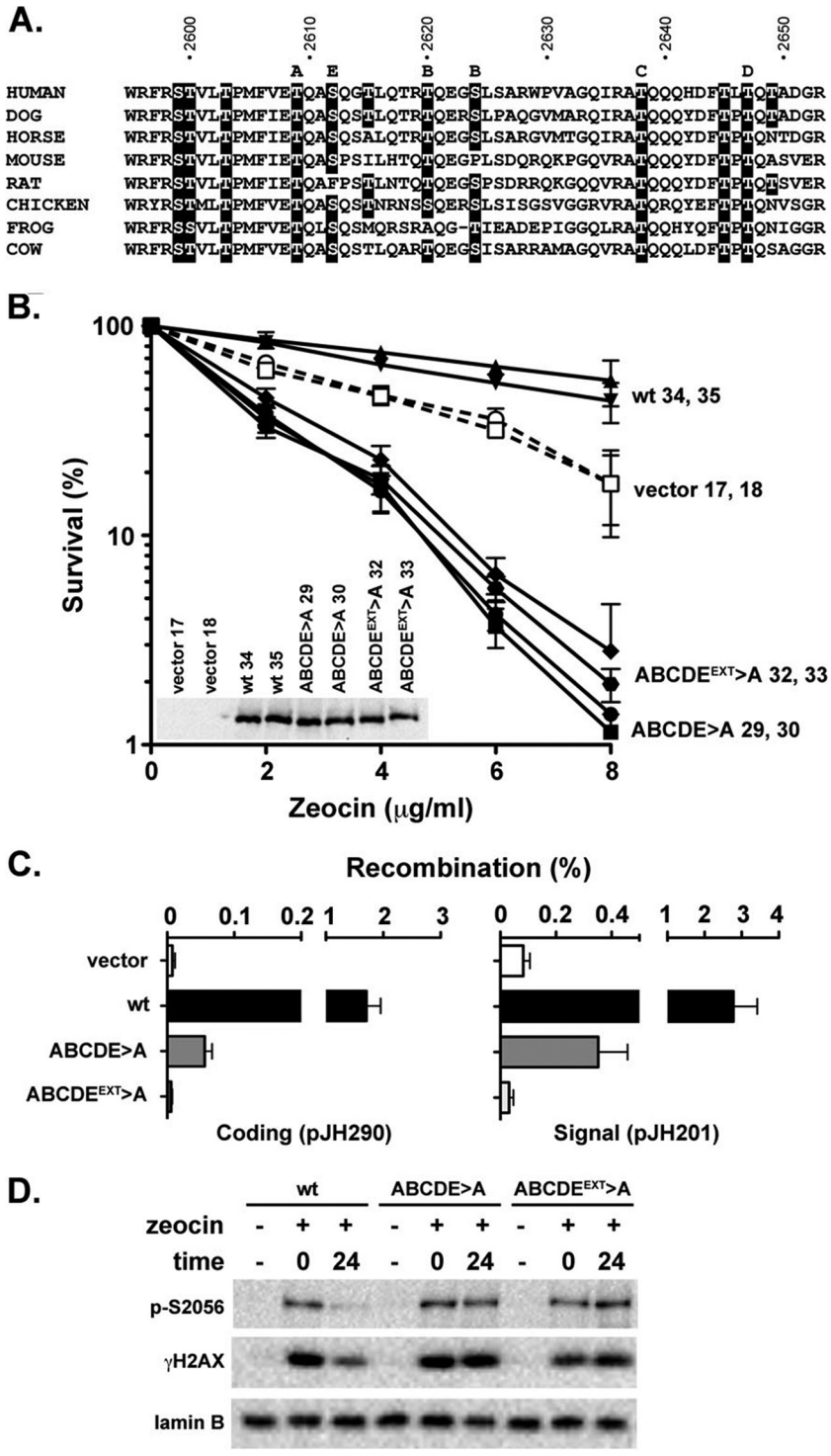

FIG 8 Blocking phosphorylation of six additional sites adjacent to the ABCDE cluster maintains the ABCDE phenotype and ablates residual VDJ activity. (A) Alignment of the DNA-PKcs amino acid sequence adjacent to the ABCDE cluster from eight species. The 12 residues that were changed to alanines in the ABCDE^{EXT} mutant are highlighted. The appropriate letter indicates the positions of the ABCDE sites. (B) Two independent V3 transfectant cell strains expressing wild-type DNA-PKcs (wt strains 34 and 35), the ABCDE>Ala mutant(strains 29 and 30), the ABCDE^{EXT}>Ala mutant(strains 32 and 33), or no DNA-PKcs (vector strains 17 and 18) were plated at cloning densities into complete medium containing increasing doses of zeocin as indicated. Colonies were stained after 7 days, and percent survival was calculated. Error bars represent standard error of the means. The inset shows the level of DNA-PKcs protein expression in untreated cells as determined by Western blotting of whole-cell extracts obtained from the indicated cell strains. (C) Recombination percentage of the coding joint substrate pJH290 or signal joint substrate pJH201 in V3 cells transiently expressing RAG proteins and either wild-type DNA-PKcs, the ABCDE>Ala mutant, the ABCDE^{EXT}>Ala mutant, or no DNA-PKcs. Error bars represent the standard error of the means. Note that the differences between the recombination efficiencies of the ABCDE>Ala and the ABCDE^{EXT}>Ala mutants for both coding end joining ($P \leq 0.001$) and signal end joining ($P \leq 0.01$) are statistically significant based on a two-tailed unpaired *t* test. (D) V3 transfectants expressing either wild type DNA-PKcs, the ABCDE>Ala mutant, or the ABCDE^{EXT}>Ala mutant were treated (or not) with 2 mg/ml zeocin for 1 h. Cells were harvested either immediately or after 24 h of culture in fresh medium. The Triton-insoluble nuclear fraction was isolated and analyzed by Western blotting for the level of expression of phospho-S2056 DNA-PKcs, γH2AX, and lamin B. One of three independent experiments performed with identical results is depicted.

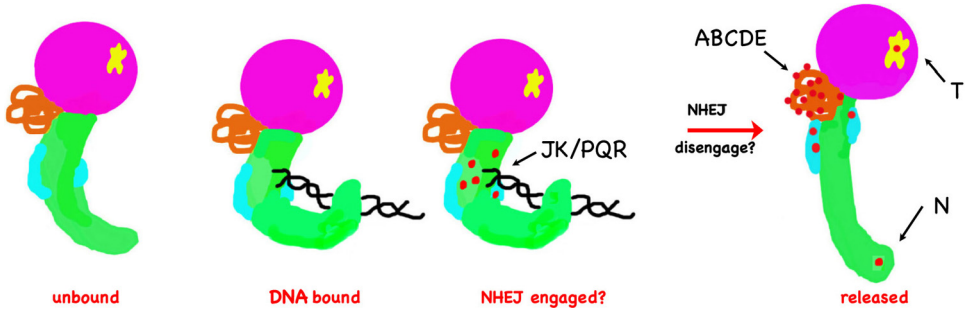

FIG 9 Model of DNA-PK conformational changes during repair. Coupled with recent structural data, our results suggest a model whereby DNA binding induces a clamping of the complex. We suggest that phosphorylations within or adjacent to the putative DNA binding domain (PQR/JK) promote initiation of NHEJ and a "clamping" of the complex. Phosphorylations of the ABCDE sites, predicted to be located in a disordered region, at a hinge between the two domains, lead to regulated, conformational changes (flattening the complex) that initially promote NHEJ and eventually disengage NHEJ. If DNA-PK is engaged (via PQR/JK phosphorylation) but can only slowly dissociate because the six ABCDE sites are blocked, c-NHEJ is slow and results in a dominant negative cellular phenotype because DNA end access is blocked from other repair factors. Maintaining catalytic activity by blocking sites that inactivate the kinase (T and N) abates this phenotype because additional sites within the ABCDE cluster ($ABCDE^{EXT}$) are more likely to be phosphorylated.

Fig. S3), suggesting that phosphorylation of these sites is also important for the dominant negative phenotype. We are continuing to investigate the potential function of these DNA-PKcs phosphorylation events.

DISCUSSION

Several conclusions can be inferred from the data presented here. First, DNA-PK binds DSBs (or unpaired double-stranded ends) that result from damage induced by a large variety of DNA damaging agents (for instance, intermediates generated by repair of DNA interstrand cross-links or DNA ends that result from replication fork arrest). Given that cells unable to phosphorylate the ABCDE sites remove cisplatin from their DNA at a lower rate than cells with or without wild-type DNA-PKcs, it seems likely that ABCDE phosphorylation is required to disengage DNA-PK (and attempted NHEJ) from those DNA ends. Consistent with this interpretation, during revision of the manuscript, Zhou and Paull reported that DNA-PK and MRN (Mre11-Rad50-Nbs1) regulate end resection and that ABCDE phosphorylation was crucial for promoting end resection (48). Understanding how DNA-PK disengages from these ends is an important, outstanding question.

Second, these studies suggest that the ABCDE>Ala mutant catalyzes defective NHEJ, which is much worse for cell viability than no NHEJ. Several published results are consistent with impaired repair by the ABCDE>Ala mutant, including the following: (i) slow resolution of DSBs (as measured by pulse-field electrophoresis [14]), (ii) increased persistence of γH2AX foci after irradiation (10), and (iii) persistent occupancy at DSBs after laser-induced damage (41, 49). The impact of DNA-PK on regulation of other DNA repair pathways is also evident in the removal of cisplatin lesions (Fig. 2). The ICP-MS methodology measures removal of all types of cisplatin-DNA damage, including intrastrand lesions, which are repaired via NER, and interstrand cross-links, which are most likely repaired via HR. The reduction in the slow repair step of the cisplatin lesions may reflect a differential impact on these various repair and tolerance pathways. Moreover, here we show that this severely impaired NHEJ requires the enzymatic activity of DNA-PK; ablating enzymatic activity in the ABCDE>Ala mutant actually reverses the observed dominant negative phenotype.

Many investigators have contributed data supporting the idea that although DNA-PK is remarkably highly phosphorylated, ABCDE phosphorylation is central to its function (7–10, 13, 16, 49). The fact that this region is predicted to lack secondary structure is a new piece of evidence further implicating phosphorylation within this region as an important molecular switch for controlling DNA-PK's function. Although the ABCDE cluster is in a region absent in the crystal structure, from modeling regions adjacent in the primary sequence, it seems likely that the ABCDE cluster is located at a hinge-like region between the head domain (FAT/kinase/FATC) and the large ring domain. Hammel et al. utilized SAXS to analyze solution structures of purified DNA-PKcs monomers that had been phosphorylated (or not) *in vitro* (41). Although *in vitro* phosphorylation of the enzyme will not result in uniform phosphorylations, we have shown previously that under these conditions, sites within the ABCDE cluster are mostly in the phosphorylated state (up to 90%) (36). SAXS structures of phosphorylated DNA-PKcs revealed dramatic conformational changes; changes occurred over the entire structure and likely resulted from relocation of DNA-PKcs domains rather than from just remodeling within domains (although changes within domains were observed as well). The most dramatic effect was "flattening" of the convex shape (as viewed from the side). The position of the ABCDE cluster at this hinge region provides a reasonable basis for implicating phosphorylation of these residues as being important for facilitating this conformational change.

Finally, based on our data as well as on previously published reports, we propose the following model (Fig. 9). Cryo-EM studies have shown that DNA-PKcs has a more crimped conformation when binding DNA. We suggest that PQR and JK phosphorylations within, or proximate to, the putative DNA binding pocket stabilize this conformation and generate an "engaged" c-NHEJ complex. Phosphorylations in the ABCDE cluster, which exists as a disordered, flexible region between the head and ring domains, promote ordered conformational changes that result in eventual flattening of the complex, consistent with the SAXS studies of Hammel et al. (41). It is tempting to speculate that the lack of secondary structure affords the $ABCDE^{EXT}$ region the ability to promote conformational changes when phosphorylated to different extents at the 12 different sites, which may explain the large impact that blocking $ABCDE^{EXT}$ phosphorylation has on the enzyme's biological function. These ordered conformational

changes could facilitate activation of Artemis, recruitment or positioning of the ligase complex, and eventual complex dissociation. Maintaining enzymatic activity, for example, by blocking kinase inactivation through phosphorylation of the N or T site, could allow phosphorylation of additional sites in the ABCDE^{EXT} cluster when the primary sites cannot be phosphorylated. If this model is correct, it follows that blocking these conformational changes must account for the severe phenotype observed in living cells when ABCDE^{EXT} phosphorylation is prohibited.

Extending this model, it is possible that different phosphorylations promote distinct conformations at different points in repair. Rivera-Calzada et al. examined DNA-PK structure after autophosphorylation by cryo-EM techniques (38). These studies examined structural features of the complete DNA-PK complex. The resulting images were remarkably heterogeneous, including heterogeneous DNA-PK dimers as well as heterogeneous Ku dimers and DNA-PKcs monomers. The heterogeneity of the images precluded assimilation of three-dimensional images of their data; consistent with the model presented here, the authors concluded that distinct autophosphorylations may result in distinct conformations and, in general, that autophosphorylation increased flexibility or plasticity in the observed complexes.

Why are these results important? The ABCDE>Ala mutant studies presented here provide a tool that has revealed that DNA-PK is targeted to DNA ends that result from many different types of DNA damaging agents in living cells. From studies presented in Fig. 1, it can be assumed that DNA-PK affects repair at collapsed replication forks and at DNA cross-links. Understanding the molecular basis of the role of DNA-PK when it is targeted to DNA ends that are likely not repairable by c-NHEJ is an important question to address. Recently, two reports demonstrated that disrupting DNA-PK in cells deficient in components of the Fanconi anemia (FA) pathway abated the FA phenotype in cells and in FA-deficient animals (50, 51). It is of considerable interest that the most prominent phenotype of the ACD>Ala mouse, in which three of the five Ser/Thr residues within the mouse ABCDE cluster have been replaced with alanines, generated by Zhang and colleagues, is bone marrow failure and, most predominately, erythrocytic lineage failure; these animals actually mimic the FA patient phenotypes better than many of the FA-deficient mice (8). These results are of particular importance if the substantial difference in DNA-PK levels present in primates versus other animals (~50-fold higher in primates) (52, 53) is considered. This may offer an explanation not only for the more dramatic phenotype in humans (versus mice) with Fanconi anemia complementation (FANC) mutations but also for the remarkably severe phenotype in the only human patient described to date with inactivating DNA-PKcs mutations (compared to the phenotypes observed in mice, dogs, and horses with inactivating DNA-PKcs mutations) (54).

ACKNOWLEDGMENTS

This work was supported by Public Health Service grant AI048758 (K.M.) and by a Canadian Institutes of Health Research Grant (MOP-89903) to M.S.J.

We especially thank undergraduate assistant Eric-John Kohler for his technical assistance throughout these studies.

REFERENCES

1. **Rothkamm K, Kruger I, Thompson LH, Lobrich M.** 2003. Pathways of DNA double-strand break repair during the mammalian cell cycle. Mol. Cell. Biol. **23:**5706–5715. http://dx.doi.org/10.1128/MCB.23.16.5706-5715.2003.
2. **Lieber MR.** 2008. The mechanism of human nonhomologous DNA end joining. J. Biol. Chem. **283:**1–5. http://dx.doi.org/10.1074/jbc.R700039200.
3. **Yan CT, Boboila C, Souza EK, Franco S, Hickernell TR, Murphy M, Gumaste S, Geyer M, Zarrin AA, Manis JP, Rajewsky K, Alt FW.** 2007. IgH class switching and translocations use a robust non-classical end-joining pathway. Nature **449:**478–482. http://dx.doi.org/10.1038/nature06020.
4. **Corneo B, Wendland RL, Deriano L, Cui X, Klein IA, Wong SY, Arnal S, Holub AJ, Weller GR, Pancake BA, Shah S, Brandt VL, Meek K, Roth DB.** 2007. Rag mutations reveal robust alternative end joining. Nature **449:**483–486. http://dx.doi.org/10.1038/nature06168.
5. **Dobbs TA, Tainer JA, Lees-Miller SP.** 2010. A structural model for regulation of NHEJ by DNA-PKcs autophosphorylation. DNA Repair (Amst.) **9:**1307–1314. http://dx.doi.org/10.1016/j.dnarep.2010.09.019.
6. **Hornbeck PV, Kornhauser JM, Tkachev S, Zhang B, Skrzypek E, Murray B, Latham V, Sullivan M.** 2012. PhosphoSitePlus: a comprehensive resource for investigating the structure and function of experimentally determined post-translational modifications in man and mouse. Nucleic Acids Res. **40:**D261–270. http://dx.doi.org/10.1093/nar/gkr1122.
7. **Chan DW, Chen BP, Prithivirajsingh S, Kurimasa A, Story MD, Qin J, Chen DJ.** 2002. Autophosphorylation of the DNA-dependent protein kinase catalytic subunit is required for rejoining of DNA double-strand breaks. Genes Dev. **16:**2333–2338. http://dx.doi.org/10.1101/gad.1015202.
8. **Zhang S, Yajima H, Huynh H, Zheng J, Callen E, Chen HT, Wong N, Bunting S, Lin YF, Li M, Lee KJ, Story M, Gapud E, Sleckman BP, Nussenzweig A, Zhang CC, Chen DJ, Chen BP.** 2011. Congenital bone marrow failure in DNA-PKcs mutant mice associated with deficiencies in DNA repair. J. Cell Biol. **193:**295–305. http://dx.doi.org/10.1083/jcb.201009074.
9. **Ding Q, Reddy YV, Wang W, Woods T, Douglas P, Ramsden DA, Lees-Miller SP, Meek K.** 2003. Autophosphorylation of the catalytic subunit of the DNA-dependent protein kinase is required for efficient end processing during DNA double-strand break repair. Mol. Cell. Biol. **23:**5836–5848. http://dx.doi.org/10.1128/MCB.23.16.5836-5848.2003.
10. **Cui X, Yu Y, Gupta S, Cho YM, Lees-Miller SP, Meek K.** 2005. Autophosphorylation of DNA-dependent protein kinase regulates DNA end processing and may also alter double-strand break repair pathway choice. Mol. Cell. Biol. **25:**10842–10852. http://dx.doi.org/10.1128/MCB.25.24.10842-10852.2005.
11. **Neal JA, Dang V, Douglas P, Wold MS, Lees-Miller SP, Meek K.** 2011. Inhibition of homologous recombination by DNA-dependent protein kinase requires kinase activity, is titratable, and is modulated by autophosphorylation. Mol. Cell. Biol. **31:**1719–1733. http://dx.doi.org/10.1128/MCB.01298-10.
12. **Neal JA, Meek K.** 2011. Choosing the right path: does DNA-PK help make the decision? Mutat. Res. **711:**73–86. http://dx.doi.org/10.1016/j.mrfmmm.2011.02.010.
13. **Soubeyrand S, Pope L, Pakuts B, Hache RJ.** 2003. Threonines 2638/2647 in DNA-PK are essential for cellular resistance to ionizing radiation. Cancer Res. **63:**1198–1201.
14. **Block WD, Yu Y, Merkle D, Gifford JL, Ding Q, Meek K, Lees-Miller SP.** 2004. Autophosphorylation-dependent remodeling of the DNA-dependent protein kinase catalytic subunit regulates ligation of DNA ends. Nucleic Acids Res. **32:**4351–4357. http://dx.doi.org/10.1093/nar/gkh761.
15. **Reddy YV, Ding Q, Lees-Miller SP, Meek K, Ramsden DA.** 2004. Nonhomologous end joining requires that the DNA-PK complex undergo an autophosphorylation-dependent rearrangement at DNA ends. J. Biol. Chem. **279:**39408–39413. http://dx.doi.org/10.1074/jbc.M406432200.
16. **Goodarzi AA, Yu Y, Riballo E, Douglas P, Walker SA, Ye R, Harer C, Marchetti C, Morrice N, Jeggo PA, Lees-Miller SP.** 2006. DNA-PK autophosphorylation facilitates Artemis endonuclease activity. EMBO J. **25:**3880–3889. http://dx.doi.org/10.1038/sj.emboj.7601255.
17. **Douglas P, Cui X, Block WD, Yu Y, Gupta S, Ding Q, Ye R, Morrice N, Lees-Miller SP, Meek K.** 2007. The DNA-dependent protein kinase catalytic subunit is phosphorylated in vivo on threonine 3950, a highly conserved amino acid in the protein kinase domain. Mol. Cell. Biol. **27:**1581–1591. http://dx.doi.org/10.1128/MCB.01962-06.
18. **Meek K, Douglas P, Cui X, Ding Q, Lees-Miller SP.** 2007. *trans* Autophosphorylation at DNA-dependent protein kinase's two major autophosphorylation site clusters facilitates end processing but not end joining. Mol. Cell. Biol. **27:**3881–3890. http://dx.doi.org/10.1128/MCB.02366-06.
19. **Chen BP, Uematsu N, Kobayashi J, Lerenthal Y, Krempler A, Yajima H,**

Lobrich M, Shiloh Y, Chen DJ. 2007. Ataxia telangiectasia mutated (ATM) is essential for DNA-PKcs phosphorylations at the Thr-2609 cluster upon DNA double strand break. J. Biol. Chem. **282:**6582–6587. http://dx.doi.org/10.1074/jbc.M611605200.

20. **Yajima H, Lee KJ, Chen BP.** 2006. ATR-dependent phosphorylation of DNA-dependent protein kinase catalytic subunit in response to UV-induced replication stress. Mol. Cell. Biol. **26:**7520–7528. http://dx.doi.org/10.1128/MCB.00048-06.
21. **Convery E, Shin EK, Ding Q, Wang W, Douglas P, Davis LS, Nickoloff JA, Lees-Miller SP, Meek K.** 2005. Inhibition of homologous recombination by variants of the catalytic subunit of the DNA-dependent protein kinase (DNA-PKcs). Proc. Natl. Acad. Sci. U. S. A. **102:**1345–1350. http://dx.doi.org/10.1073/pnas.0406466102.
22. **Kienker LJ, Shin EK, Meek K.** 2000. Both V(D)J. recombination and radioresistance require DNA-PK kinase activity, though minimal levels suffice for V(D)J. recombination. Nucleic Acids Res. **28:**2752–2761. http://dx.doi.org/10.1093/nar/28.14.2752.
23. **Shin EK, Rijkers T, Pastink A, Meek K.** 2000. Analyses of TCRB rearrangements substantiate a profound deficit in recombination signal sequence joining in SCID foals: implications for the role of DNA-dependent protein kinase in V(D)J. recombination. J. Immunol. **164:**1416–1424.
24. **Drouet J, Delteil C, Lefrancois J, Concannon P, Salles B, Calsou P.** 2005. DNA-dependent protein kinase and XRCC4-DNA ligase IV mobilization in the cell in response to DNA double strand breaks. J. Biol. Chem. **280:**7060–7069. http://dx.doi.org/10.1074/jbc.M410746200.
25. **Hesse JE, Lieber MR, Gellert M, Mizuuchi K.** 1987. Extrachromosomal DNA substrates in pre-B cells undergo inversion or deletion at immunoglobulin V-(D)-J. joining signals. Cell **49:**775–783. http://dx.doi.org/10.1016/0092-8674(87)90615-5.
26. **Laird PW, Zijderveld A, Linders K, Rudnicki MA, Jaenisch R, Berns A.** 1991. Simplified mammalian DNA isolation procedure. Nucleic Acids Res. **19:**4293. http://dx.doi.org/10.1093/nar/19.15.4293.
27. **McGuffin LJ, Bryson K, Jones DT.** 2000. The PSIPRED protein structure prediction server. Bioinformatics **16:**404–405. http://dx.doi.org/10.1093/bioinformatics/16.4.404.
28. **Soding J, Biegert A, Lupas AN.** 2005. The HHpred interactive server for protein homology detection and structure prediction. Nucleic Acids Res. **33:**W244–W248. http://dx.doi.org/10.1093/nar/gki408.
29. **Sibanda BL, Chirgadze DY, Blundell TL.** 2010. Crystal structure of DNA-PKcs reveals a large open-ring cradle comprised of HEAT repeats. Nature **463:**118–121. http://dx.doi.org/10.1038/nature08648.
30. **Schwartz M, Zlotorynski E, Goldberg M, Ozeri E, Rahat A, le Sage C, Chen BP, Chen DJ, Agami R, Kerem B.** 2005. Homologous recombination and nonhomologous end-joining repair pathways regulate fragile site stability. Genes Dev. **19:**2715–2726. http://dx.doi.org/10.1101/gad.340905.
31. **Pluth JM, Fried LM, Kirchgessner CU.** 2001. Severe combined immunodeficient cells expressing mutant hRAD54 exhibit a marked DNA double-strand break repair and error-prone chromosome repair defect. Cancer Res. **61:**2649–2655.
32. **Song Q, Lees-Miller SP, Kumar S, Zhang Z, Chan DW, Smith GC, Jackson SP, Alnemri ES, Litwack G, Khanna KK, Lavin MF.** 1996. DNA-dependent protein kinase catalytic subunit: a target for an ICE-like protease in apoptosis. EMBO J. **15:**3238–3246.
33. **Han Z, Malik N, Carter T, Reeves WH, Wyche JH, Hendrickson EA.** 1996. DNA-dependent protein kinase is a target for a CPP32-like apoptotic protease. J. Biol. Chem. **271:**25035–25040. http://dx.doi.org/10.1074/jbc.271.40.25035.
34. **Lee GS, Neiditch MB, Salus SS, Roth DB.** 2004. RAG proteins shepherd double-strand breaks to a specific pathway, suppressing error-prone repair, but RAG nicking initiates homologous recombination. Cell **117:**171–184. http://dx.doi.org/10.1016/S0092-8674(04)00301-0.
35. **Gupta S, Meek K.** 2005. The leucine rich region of DNA-PKcs contributes to its innate DNA affinity. Nucleic Acids Res. **33:**6972–6981. http://dx.doi.org/10.1093/nar/gki990.
36. **Douglas P, Sapkota GP, Morrice N, Yu Y, Goodarzi AA, Merkle D, Meek K, Alessi DR, Lees-Miller SP.** 2002. Identification of in vitro and in vivo phosphorylation sites in the catalytic subunit of the DNA-dependent protein kinase. Biochem. J. **368:**243–251. http://dx.doi.org/10.1042/BJ20020973.
37. **Spagnolo L, Rivera-Calzada A, Pearl LH, Llorca O.** 2006. Three-dimensional structure of the human DNA-PKcs/Ku70/Ku80 complex assembled on DNA and its implications for DNA DSB repair. Mol. Cell **22:**511–519. http://dx.doi.org/10.1016/j.molcel.2006.04.013.
38. **Rivera-Calzada A, Maman JD, Spagnolo L, Pearl LH, Llorca O.** 2005. Three-dimensional structure and regulation of the DNA-dependent protein kinase catalytic subunit (DNA-PKcs). Structure **13:**243–255. http://dx.doi.org/10.1016/j.str.2004.12.006.
39. **Llorca O, Pearl LH.** 2004. Electron microscopy studies on DNA recognition by DNA-PK. Micron **35:**625–633. http://dx.doi.org/10.1016/j.micron.2004.05.004.
40. **Boskovic J, Rivera-Calzada A, Maman JD, Chacon P, Willison KR, Pearl LH, Llorca O.** 2003. Visualization of DNA-induced conformational changes in the DNA repair kinase DNA-PKcs. EMBO J. **22:**5875–5882. http://dx.doi.org/10.1093/emboj/cdg555.
41. **Hammel M, Yu Y, Mahaney BL, Cai B, Ye R, Phipps BM, Rambo RP, Hura GL, Pelikan M, So S, Abolfath RM, Chen DJ, Lees-Miller SP, Tainer JA.** 2010. Ku and DNA-dependent protein kinase dynamic conformations and assembly regulate DNA binding and the initial non-homologous end joining complex. J. Biol. Chem. **285:**1414–1423. http://dx.doi.org/10.1074/jbc.M109.065615.
42. **Babu MM, van der Lee R, de Groot NS, Gsponer J.** 2011. Intrinsically disordered proteins: regulation and disease. Curr. Opin. Struct. Biol. **21:**432–440. http://dx.doi.org/10.1016/j.sbi.2011.03.011.
43. **Bennetzen MV, Larsen DH, Bunkenborg J, Bartek J, Lukas J, Andersen JS.** 2010. Site-specific phosphorylation dynamics of the nuclear proteome during the DNA damage response. Mol. Cell. Proteomics **9:**1314–1323. http://dx.doi.org/10.1074/mcp.M900616-MCP200.
44. **Bensimon A, Schmidt A, Ziv Y, Elkon R, Wang SY, Chen DJ, Aebersold R, Shiloh Y.** 2010. ATM-dependent and -independent dynamics of the nuclear phosphoproteome after DNA damage. Sci. Signal. **3:**rs3. http://dx.doi.org/10.1126/scisignal.2001034.
45. **Chan DW, Lees-Miller SP.** 1996. The DNA-dependent protein kinase is inactivated by autophosphorylation of the catalytic subunit. J. Biol. Chem. **271:**8936–8941. http://dx.doi.org/10.1074/jbc.271.15.8936.
46. **Olsen JV, Vermeulen M, Santamaria A, Kumar C, Miller ML, Jensen LJ, Gnad F, Cox J, Jensen TS, Nigg EA, Brunak S, Mann M.** 2010. Quantitative phosphoproteomics reveals widespread full phosphorylation site occupancy during mitosis. Sci. Signal. **3:**ra3. http://dx.doi.org/10.1126/scisignal.2000475.
47. **Dephoure N, Zhou C, Villen J, Beausoleil SA, Bakalarski CE, Elledge SJ, Gygi SP.** 2008. A quantitative atlas of mitotic phosphorylation. Proc. Natl. Acad. Sci. U. S. A. **105:**10762–10767. http://dx.doi.org/10.1073/pnas.0805139105.
48. **Zhou Y, Paull TT.** 2013. DNA-dependent Protein Kinase regulates DNA end resection in concert with the Mre11-Rad50-Nbs1 (MRN) complex and ataxia-telangiectasia-mutated (ATM). J. Biol. Chem. **288:**37112–37125. http://dx.doi.org/10.1074/jbc.M113.514398.
49. **Shibata A, Conrad S, Birraux J, Geuting V, Barton O, Ismail A, Kakarougkas A, Meek K, Taucher-Scholz G, Lobrich M, Jeggo PA.** 2011. Factors determining DNA double-strand break repair pathway choice in G_2 phase. EMBO J. **30:**1079–1092. http://dx.doi.org/10.1038/emboj.2011.27.
50. **Pace P, Mosedale G, Hodskinson MR, Rosado IV, Sivasubramaniam M, Patel KJ.** 2010. Ku70 corrupts DNA repair in the absence of the Fanconi anemia pathway. Science **329:**219–223. http://dx.doi.org/10.1126/science.1192277.
51. **Adamo A, Collis SJ, Adelman CA, Silva N, Horejsi Z, Ward JD, Martinez-Perez E, Boulton SJ, La Volpe A.** 2010. Preventing nonhomologous end joining suppresses DNA repair defects of Fanconi anemia. Mol. Cell **39:**25–35. http://dx.doi.org/10.1016/j.molcel.2010.06.026.
52. **Finnie NJ, Gottlieb TM, Blunt T, Jeggo PA, Jackson SP.** 1995. DNA-dependent protein kinase activity is absent in xrs-6 cells: implications for site-specific recombination and DNA double-strand break repair. Proc. Natl. Acad. Sci. U. S. A. **92:**320–324. http://dx.doi.org/10.1073/pnas.92.1.320.
53. **Lees-Miller SP, Sakaguchi K, Ullrich SJ, Appella E, Anderson CW.** 1992. Human DNA-activated protein kinase phosphorylates serines 15 and 37 in the amino-terminal transactivation domain of human p53. Mol. Cell. Biol. **12:**5041–5049.
54. **Woodbine L, Neal JA, Sasi NK, Shimada M, Deem K, Coleman H, Dobyns WB, Ogi T, Meek K, Davies EG, Jeggo PA.** 2013. PRKDC mutations in a SCID patient with profound neurological abnormalities. J. Clin. Invest. **123:**2969–2980. http://dx.doi.org/10.1172/JCI67349.